Available online at www.sciencedirect.com
SCIENCE DIRECT®
Sensors and Actuators B 105 (2005) 251–258
SENSORS AND ACTUATORS B CHEMICAL
www.elsevier.com/locate/snb

A microchip-based PCR device using flexible printed circuit technology

Keyue Shen [a,b], Xiaofang Chen [a,b], Min Guo [b], Jing Cheng [a,b,c,*]

[a] *Department of Biological Sciences and Biotechnology, Tsinghua University, Beijing 100084, China*
[b] *National Engineering Research Center for Beijing Biochip Technology, 18 Life Science Parkway, Changping District, Beijing 102206, China*
[c] *State Key Laboratory of Biomembrane and Membrane Biotechnology, Tsinghua University, Beijing 100084, China*

Received 13 February 2004; received in revised form 26 May 2004; accepted 27 May 2004
Available online 22 July 2004

Abstract

Rapid heat transfer is crucial for an efficient polymerase chain reaction (PCR), and this makes temperature control one of the most essential features in a micro-PCR system, which always includes a heater and a sensor composing a closed-loop. Yet, the fabrication of the heater and the sensor often prevented micro-PCR systems from achieving both cost-effectiveness and fabrication-easiness. For most of the early researches micromachining techniques were used to allow sensors and heaters be integrated on a silicon or glass chip. However, the cost prevented them from wide applications. The work described in this paper is part of our effort to solve the cost/fabrication dilemma. An innovative digital temperature control system was developed by introducing a heater/sensor switching procedure. Only one temperature controlling element fabricated by flexible printed circuit technology was utilized in the constructed PCR device with minimum fabrication steps. The glass chip-based device was made from low cost materials and assembled with adhesive bonding. Through seemingly simple steps, we obtained both disposability and portability at the same time. Temperature stability within ±0.3 °C and a transitional rate of 8 °C/s during heating/cooling was achieved. A 244 bp DNA fragment of hepatitis C virus was successfully amplified in our device by a three-stage thermal cycling process. Further improvement was assisted by finite element analysis, and demonstrated by experiment.
© 2004 Elsevier B.V. All rights reserved.

Keywords: Micro-PCR; Thermal component; Flexible printed circuit (FPC); Finite element analysis (FEA)

1. Introduction

Polymerase chain reaction (PCR) has been playing a central role in nucleic acid analyses since 1983. It is a temperature controlled and enzyme-mediated amplification technique for nucleic acid molecules, usually consisting of periodical repetition of three reaction steps: a denaturing step at 92–96 °C, an annealing step at 37–65 °C (determined by the inherent nucleic acid sequences) and an extending step at ∼72 °C.

The basic requirement for an efficient amplification is rapid heat transfer [1]. Consequently, it is desirable to have a device with a low thermal capacity and high heat conductivity. For most of the traditional PCR instruments, the heating and cooling rates were slow because of their relative large thermal components. Miniaturization of conventional PCR devices could bring in great saving in space, time and reagents, and accelerate the amplification process by increasing the surface to volume ratio [2].

In general, a micro-PCR system should be composed of two functional parts: a fabricated three-dimensional structure and a temperature control system.

Early development of silicon-based micro-PCR devices were facilitated by the micro-fabrication technology [3–5]. Silicon was preferred because of its high thermal conductivity and controllable etching properties. This material is not transparent, and untreated silicon may cause inhibition to PCR [6]. Glass has the advantage of being electrically nonconductive and optically transparent. Yet, it is not as amenable as silicon in micromachining. Moreover, fabrication of silicon/glass structures usually involves processes such as photolithography, wet etching, electrochemical etching and anodic bonding. The high costs of these processes cannot accommodate the disposability required by PCR reactions to avoid cross-contamination. Recently, plastic materials are more popular for its ease of use, low cost and disposability, and there are many established techniques for building complex structures. For example, polycarbonate

* Corresponding author. Tel.: +86-10-62772239; fax: +86-10-80726898.
E-mail address: jcheng@tsinghua.edu.cn (J. Cheng).

0925-4005/$ – see front matter. © 2004 Elsevier B.V. All rights reserved.
doi:10.1016/j.snb.2004.05.069

and poly(cyclic olefin) have been employed in micro-PCR devices [7,8]. Also, the surface of many plastics is biocompatible. Although the lower thermal conductivity makes them less sufficient for thermal cycling, the influence can be minimized by reducing the thickness on thermal paths [9].

Temperature control is an essential feature in micro-PCR. It includes software (control method) and hardware (sensors and heaters). Most researchers preferred proportional–integral–differential control [7,10,11], while others adopted the on–off approach [12]. For those systems, a heater and a sensor are usually required to form a closed-loop. Thus, there are two opposite approaches: to fabricate both the sensor and heater on a single chip, or to assemble those two discrete components after fabrication. In silicon/glass based designs, resistive heaters and sensors can be easily mounted using thin-film techniques such as plasma enhanced chemical vapor deposition. However, the cost is prohibitive. Among plastic-based devices, researchers often use independent thermal components, such as thermoelectric (TE, or Peltier) heater/cooler, thermocouple and resistive thermal devices, to avoid micromachining. Although disposable, the fabrication steps for plastics are still complicated, and their portability and efficiency are not as competitive as micro-machined ones. Moreover, it is difficult to achieve good thermal contact among the surfaces of the target region, the sensor and the heater, which may result in the reliability problems [7].

In our work, an innovative control method was developed to solve this cost/fabrication dilemma. A resistive thermal component was designed utilizing flexible printed circuit (FPC) technology, and a novel digital temperature control system was established to drive the component both as a heater and a sensor. Using adhesive bonding, we constructed a low-cost and disposable plastic-glass hybrid-type micro-PCR device in a sandwich structure. Temperature transitional rate of 8 °C/s was achieved during heating and cooling, allowing rapid and successful PCR experiments to be performed. A 244 bp DNA fragment of hepatitis C virus (HCV) was amplified by a three-stage (94, 55 and 72 °C) thermal cycling process on the chip-based device. Further structural improvement was facilitated using finite element analysis (FEA) and its effectiveness was experimentally demonstrated.

2. Design

2.1. Resistive thermal component

Today, flexible circuits are used in nearly all kinds of electrical and electronic products. A flexible printed circuit is a patterned arrangement of printed wiring utilizing flexible base material with or without flexible cover layers. Flexible circuits are most commonly manufactured using one of two base materials, i.e., polyimide or polyester. The single-sided FPC technology was used to construct the thermal component. Single-sided flexible circuits are most commonly seen in mass production today. The construction consists of a single patterned conductor layer on a flexible dielectric film. Termination features on these circuits are accessible only from one side. Many different metal foils can be used as the conductor, and copper foil is the most commonly used one.

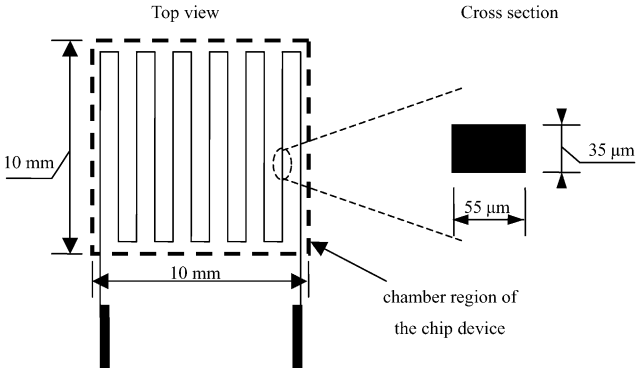

Fig. 1. Schematic design of the resistive thermal component and its cross-sectional view.

There are numerous advantages for using FPC technology, e.g., reduced size, weight, assembly time and cost. However, the most important one lies in its improved heat dissipation capability. Flat conductors have a much greater surface-to-volume ratio than round wire, allowing the efficient dissipation of heat in conductors. More over, the short thermal path in flex circuit constructions could help to further improve heat dissipation.

Fig. 1 is the schematic design of the thermal component. The resistive serpentine copper wire was mounted between two polyimide films to form a film heater using the FPC technology. The cross-section of the wire is a rectangle with a height of 35 μm and width 55 μm. According to the theory of the electrical circuits, power P generated by a resistor can be expressed as

$$P = \frac{U^2}{R} \tag{1}$$

where R is the resistance and U the applied voltage. In this design, the resistance of the film heater is approximately 3.0 Ω. Theoretically, when a low voltage, 12 V for example, is applied, the heater can generate an instantaneous maximum heating power of up to 48 W. It is ideal for applications using portable low power supplies to obtain a fast temperature ramping rate.

For most materials, their resistances change with the temperature due to the temperature dependence of the resistivity and the thermal expansion of the conductor. For copper, its thermal expansion effect is at least 200 times smaller than the effect of the resistivity change. Therefore, the thermal expansion effect can often be ignored. From 30 to 95 °C in this work, the overall resistance is a linear function of the temperature, T, and can be expressed as

$$R(T) = R(T_0)[1 + \alpha(T - T_0)] \tag{2}$$

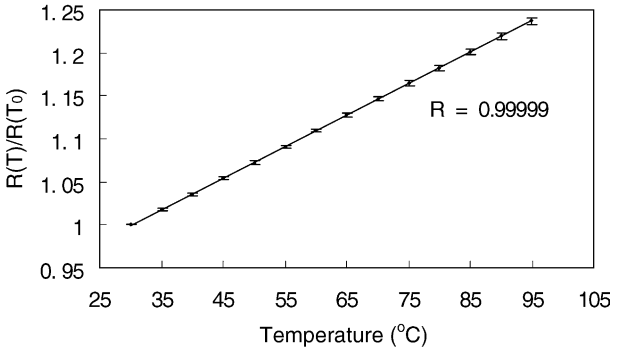

Fig. 2. Linear relationship between temperature and the relative resistance of six copper-wire resistive thermal components, and R is the correlation coefficient.

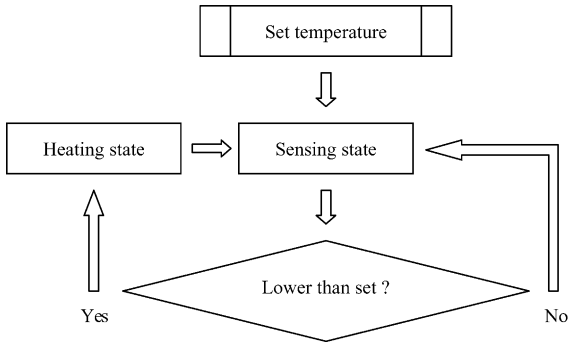

Fig. 3. Flow chart of the heater/sensor switching-based temperature control method.

where T_0 is the reference temperature (°C), T the temperature of interest (°C), $R(T_0)$ the resistance at reference temperature (Ω), $R(T)$ the resistance at temperature of interest (Ω), and α the temperature coefficient of resistivity (1/°C). Therefore, the component can also work as a sensor by calculating the temperature from the measured resistance of a serpentine copper wire. Fig. 2 shows the measured linear relationship between the temperature and the relative resistance of six thermal components. The components were put in a waterbath (Model 12101-15, Polystat® Constant Temperature Circulator, Cole Parmer Instrument Company, Vernon Hills, IL). The resistance was measured by a sourcemeter (Keithley 2400 Sourcemeter, Keithley Instruments, Cleveland, OH). A high linearity was observed in the temperature range from 30 to 95 °C.

2.2. Temperature control system

The idea of achieving both heater and sensor in a single component is not uncommon, but usually not practical in precision temperature control. Indium-tin oxide (ITO) was used to make the heating film in capillary PCR chip [10]. The voltage drop across and current flow through the ITO film were measured, and its resistance was calculated in real-time. Unfortunately, the experiments showed that operating the ITO film as a sensor requests a minimum current flow during cooling, which slows down the cooling rate due to its large resistance of about 525 Ω. Moreover, driving the film as a heater introduced additional resistance fluctuations which further limited the measurement accuracy of temperature to ±10 °C.

With our design, it is a great advantage that the resistance of the thermal component is small. In a practical operation a constant current flow of 10 mA was applied, and the voltage drop measured which is linear with the resistance. The total power consumption is 0.3 mW, which is too small to affect or slow down the cooling rate.

To achieve both functions of a sensor and a heater with one component, it is highly desired to allow the component playing different roles over time to avoid interferences introduced by heating current. At any time during operation, the component is either in a “heating state” (H) or a “sensing state” (S) (the S state is also a passive natural cooling period). The length of the two states can be determined independently. The temperature status of the former period determines what role the component may play in the followed stage. According to this principle, the control program can be described as follows:

(1) If the current state is H, then the next one must be S,
(2) If the current state is S, then compare the measured temperature with the set value. If it is lower than the latter, the next state will then be H; otherwise remains at S.

By obeying these two simple rules, a precision temperature control can be achieved. Fig. 3 shows the flow chart of the temperature control method with the heater/sensor switching mechanism.

The constant current flow was generated by a voltage reference (MAX6325, Maxim Integrated Products, Sunnyvale, CA). The voltage drop on the component was amplified by an op-amp (OP-07, Maxim Integrated Products, Sunnyvale, CA). The heater/sensor switching was accomplished by a power MOSFET (IRF9640, Fairchild Semiconductor, South Portland, ME). LabVIEW program was used for temperature control in thermal cycling. It communicates with the control circuit through a data acquisition (DAQ) card (AT-MIO-16E-10, National Instruments, Austin, TX). The cooling air was provided by a 12 V dc turbo fan (Model BFB1012M, Delta Electronics, Beijing, China).

Fig. 4 shows the diagram of the temperature measurement and the control system. The LabVIEW program initiates the DAQ card consisting of analog/digital (A/D) converters and digital input/output (I/O) ports. During S state, the voltage drop on the thermal component is amplified and acquired through an A/D converter. Following the two control rules, the program makes calculations and decides what state the next step will be. When an H state is selected, the MOSFET is switched on, and a heating voltage is applied to the thermal component. Otherwise, S state continues and the program repeats the data acquisition step.

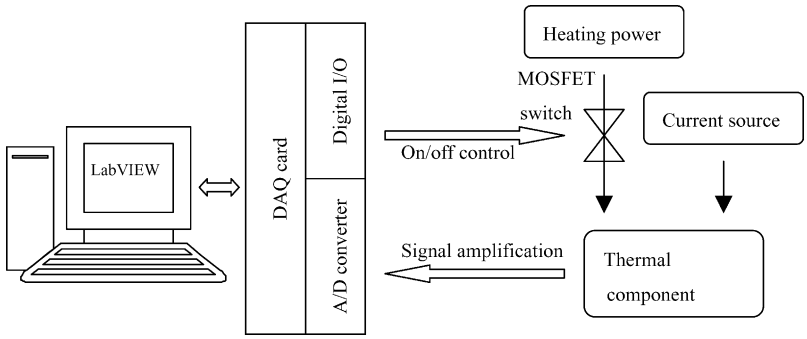

Fig. 4. The diagram of temperature measurement and control system.

3. Chip device

3.1. Fabrication

Adhesive tape bonding is one of the primary bonding techniques used in device assembly. Usually the adhesive on tapes are not biologically compatible with PCR reactions. Gene Frame® (AB0576, ABgene, Rochester, NY) was chosen to assemble the PCR chambers mainly because we found that it can withstand temperatures of up to 97 °C and shows no inhibition to PCR reactions.

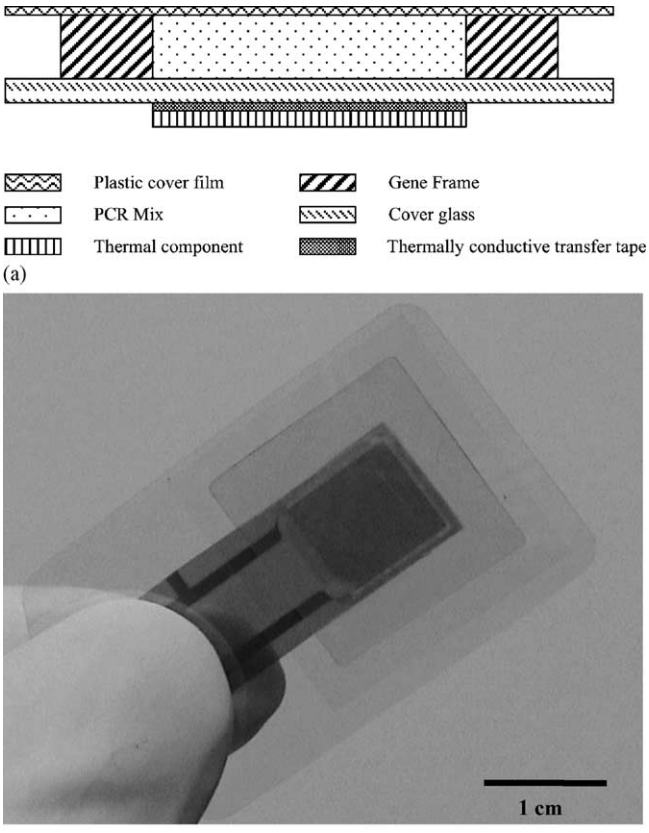

Fig. 5. The schematic structure of chip device (a) and an assembled micro-PCR chip (b).

The structure of the chip-based micro-PCR device is shown in Fig. 5. A Gene Frame® double-sided tape (250 μm thick) with a pre-punched hole in the middle was sandwiched between a 22 mm × 22 mm × 150 μm cover glass (Erie Scientific, Portsmouth, NH) and a 25 mm × 40 mm × 50 μm plastic film, forming PCR chamber with a volume of 25 μL. The film heater was attached to the backside of the cover glass using a thermally conductive transfer tape (50 μm thick, Model 9882, 3 M, Minneapolis, MN).

3.2. Calibration

To guarantee the accuracy in temperature measurement, the relationship between the measured voltage (which shows the resistance of thermal component) and the temperature in PCR chamber was calibrated by placing a T-type thermocouple in the middle of the PCR chamber (Fig. 6a). The relationship between the measured voltage on thermal com-

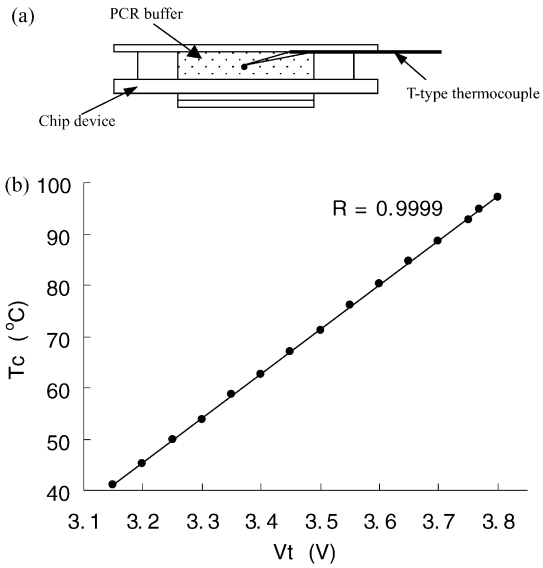

Fig. 6. The calibration method (a) and the relationship between sensed and amplified voltage drop on thermal component and chamber temperature (b). The solid line is the result of least square fitting according to the experimental data, and *R* is its correlation coefficient.

ponent (V_t, V) and the temperature inside the chamber (T_c, °C) are shown in Fig. 6b. Using the least square fitting, this relationship can be represented by the following linear equation:

$$T_c = A + BV_t \quad (3)$$

where A is −231.67 °C and B is 86.58 °C/V in the experiment. According to the thermocouple measurements, the maximum variations around the set temperatures were within ±0.3 °C. The linear relationship was used for setting temperatures in PCR programs.

4. Experiments

4.1. Reagents

Reagent kits *Taq* MasterMix (2×) for PCR amplification were purchased from Tianwei Biotech (Beijing, China). The hepatitis C virus DNA cloned into the T-vector was used as the template for PCR reaction (pHCV244, Capital Biochip, Beijing, China). The sequence information of primer set used to amplify the 244 bp target segment is 5′CTC GCA AGC ACC CTA TCA GGC AGT3′ (forward) and 5′GCA GAA AGC GTC TAG CCA TGG CGT3′ (reverse).

4.2. PCR amplification

The total reaction volume was 25 μL including 5 ng plasmid, 10 mmol/L Tris–HCl (pH 8.3 at 24 °C), 50 mmol/L KCl, 1.5 mmol/L $MgCl_2$, 0.5 μmol/L each primer, and 2.5 unit *Taq* DNA polymerase, 250 μmol/L each deoxynucleoside triphosphate and 0.005% bovine serum albumin.

Prior to the chip-based PCR, the PCR chips filled with samples were thermal-cycled on the Slide Griddle™ (Model SGP-0196, MJ Research, South San Francisco, CA) in a commercial thermal cycler (Model PTC-225, MJ Research) to test the PCR compatibility of the internal surface of the chamber. The temperature program for Slide Griddle™ and its control was kept the same: 30 cycles at 94 °C for 30 s, 55 °C for 30 s, and 72 °C for 60 s, including an initial denature step, 94 °C for 180 s and a final extension step of 72 °C for 600 s.

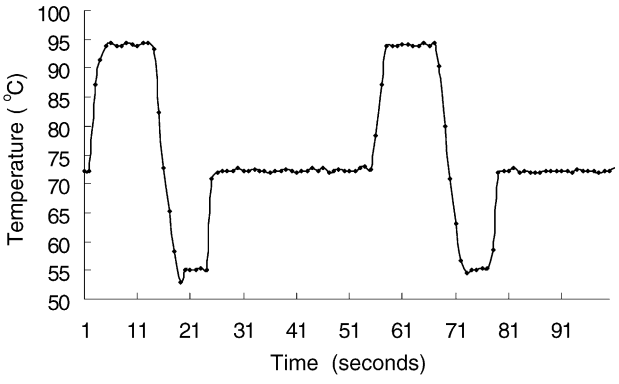

Fig. 7. The recording of the thermal cycling in 100 s.

Thermal cycling conditions for micro-PCR on chip were as follows: one cycle at 94 °C for 30 s; 30 cycles at 94 °C for 10 s, 55 °C for 5 s, and 72 °C for 30 s; one cycle at 72 °C for 60 s. The cycle was completed in 28 min. Fig. 7 shows the cycling data of 100 s. Amplifications in Eppendorf tubes in a MJ PTC-225 thermal cycler were used as controls. The temperature setting was programmed same as that for the film heater, and the cycle was completed in 70 min.

5. Results and discussion

5.1. PCR results and temperature distribution

All PCR products were electrophoresed on a 1.0% agarose gel along with commercial DNA reference ladders (see Figs. 8 and 9). The successful amplification performed in chip-based devices on commercial thermal cycler proved that the internal surface of the chamber did not cause noticeable inhibition to PCR reactions (Fig. 8). The PCR

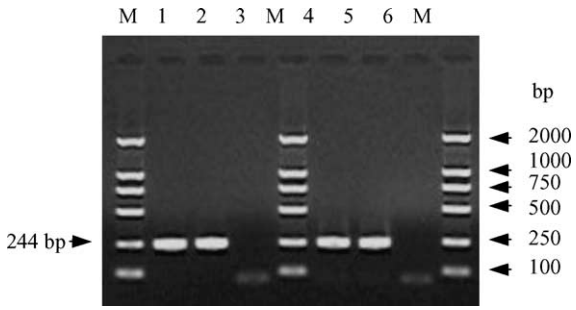

Fig. 8. Agarose gel (1.0% in 1× TAE) electrophoresis of the PCR products amplified in the MJ PTC-225 thermal cycler. Lane M: DL2000 marker (TaKaRa Bio-Company, Shiga, Japan). Lanes 1, 2: reference PCR performed in Eppendorf tubes in MJ thermal cycler. Lanes 4, 5: reference PCR performed in micro-PCR devices on Slide GriddleTM in MJ thermal cycler. Lanes 3, 6: negative control, the same mixtures without DNA template was used for PCR amplification under each condition.

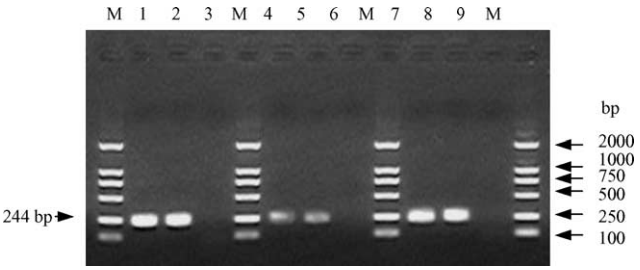

Fig. 9. Agarose gel (1.0% in 1× TAE) electrophoresis of the PCR products. Lane M: DL2000 marker (TaKaRa Bio-Company, Shiga, Japan). Lanes 1, 2: reference PCR performed in Eppendorf tubes on MJ PTC-225 thermal cycler. Lanes 4, 5: products performed in chip devices using thermal component. Lanes 7, 8: products generated in improved micro-PCR devices using thermal component. Lanes 3, 6, 9: negative control, the same mixtures without DNA template was used for PCR amplification under each condition.

amplification performed using the film heater generated the expected amplicon with a size of 244 bp (lanes 4 and 5 in Fig. 9), with yields lower than that of the controls (lanes 1 and 2 in Fig. 9).

Temperature distribution inside the reaction chamber was a crucial factor to explain the low efficiency, but its measurement was hard to take. In contacting measurements, due to the small thermal mass of the chip, the load effect of an external thermometer will greatly affect the temperature distribution, thus make the measurement inaccurate. There are some non-contact measurements, e.g., infrared radiation photos and temperature-dependent fluorescent dyes [13]. However, the former can only provide the surface temperature pattern and the latter requires transparency, which prevents many kinds of materials from being employed in chip fabrication. FEA is a powerful mathematics tool to solve this problem. It has been used in the analysis of temperature for micro-PCR [4,9,14]. In our work, the temperature distribution in the current micro-PCR device was simulated using FEA software ANSYS 7.0 (ANSYS Inc., Canonsburg, PA).

A three-dimensional model is built for steady state analysis, and the dimensions are the same as the real device. Conduction and convection are considered. Natural convection film coefficient of air is usually 1–10 W/m^2 K, and in all analysis in this paper, it is set to 3 W/m^2 K with environmental air temperature at 25 °C. The material parameters are shown in Table 1. We used the denaturing step as an extreme situation where the maximum temperature gradient is obtained during PCR. Temperature distributions of the whole chip and the chamber are shown in Fig. 10 (the power consumption was 0.096 W). A temperature difference of up to ~25 °C is observed in the chamber because of the low thermal conductivity of the substrate materials. It also implies that the temperature measured by the thermal component is a mean value. The widely-varied temperature distribution may not only reduce the PCR efficiency but also produce non-specific amplifications.

5.2. Structural improvement and validation

The problem of large temperature distribution in reaction chamber is not prevailing in silicon-based designs due to its excellent thermal conductivity (150 W/m K). In the current work, we have solved the problem by attaching a 12 mm × 12 mm × 50 μm copper chip on the backside of the chip device (Fig. 11). Copper has a good thermal conductivity of 397 W/m K, better than silicon. Fig. 12 shows the result of

Table 1
Material parameters for ANSYS analysis

	Adhesive tape	Glass	Copper	Water	Air	Plastic
Conductivity coefficient (W/m K)	0.6	1.05	397	0.628	0.024	0.2

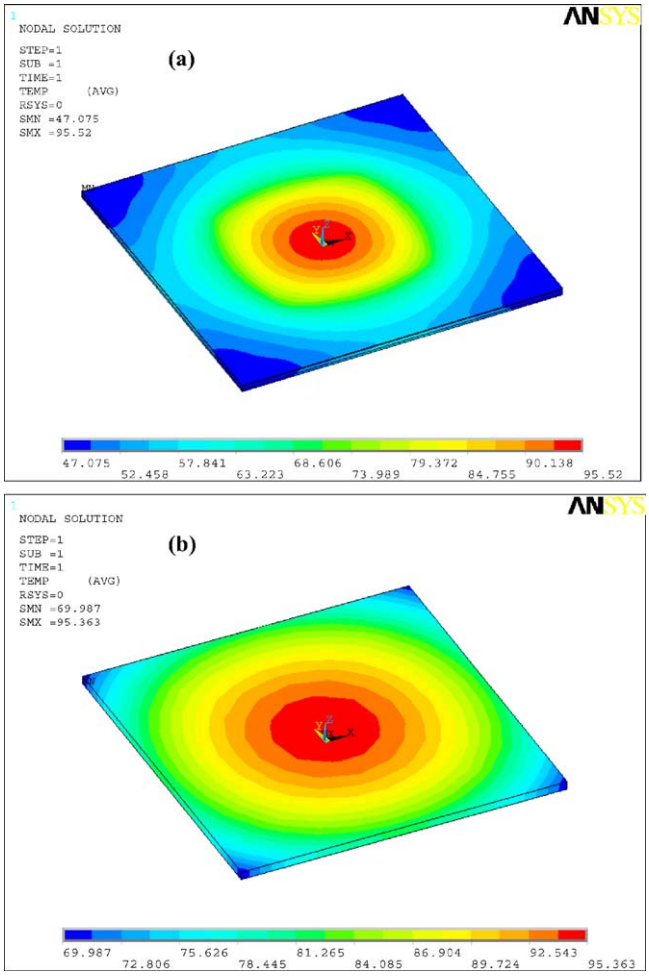

Fig. 10. Simulated temperature distribution of the micro-PCR device (steady state): the overall temperature distribution (a) and temperature distribution in the chamber (b).

simulation. Temperature difference inside the chamber was reduced significantly to 0.93 °C, which can be regarded as uniform. The temperature uniformity is achieved at the cost of relatively higher power consumption (0.135 W) and lower heating rate (4 °C/s). PCR reactions were performed and the products are shown in lanes 7 and 8 in Fig. 9. Good agreement between modeling prediction and the experimental data was obtained. The amplification efficiency was greatly improved to compete with the results of the commercial ther-

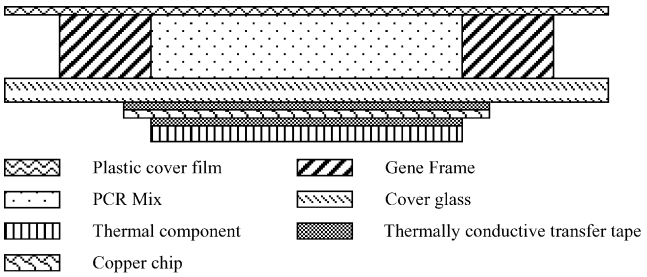

Fig. 11. The improved design of the micro-PCR device.

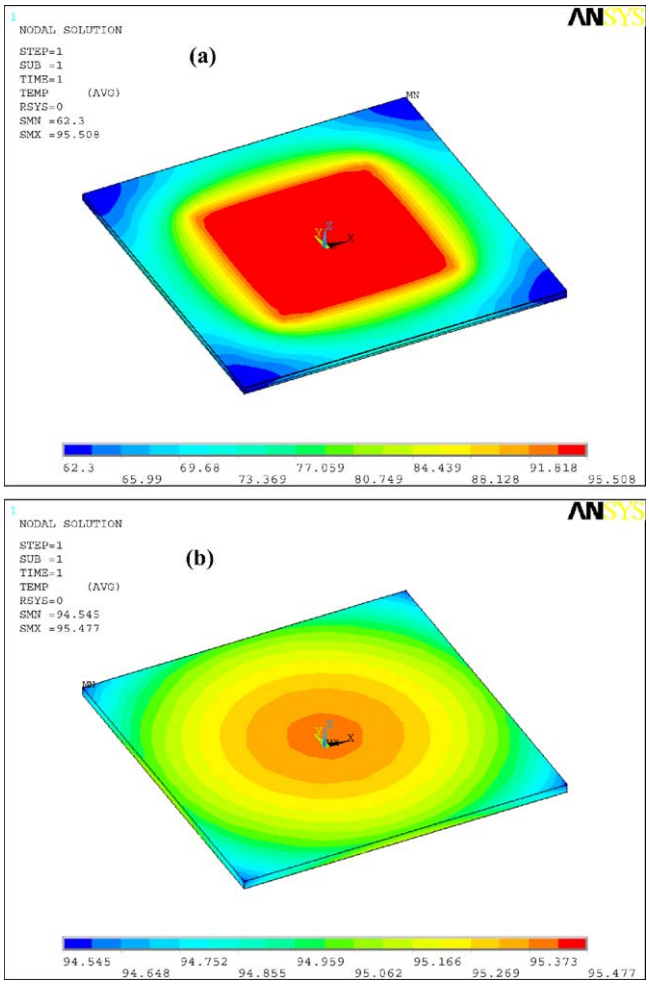

Fig. 12. Simulated temperature distribution of the improved micro-PCR device with copper chip (steady state): the overall temperature distribution (a) and temperature distribution in the chamber (b).

mal cycler, yet the total reaction time was 30 min, only 2 min longer than the previous design.

5.3. Thermal component and temperature control

The thermal mass of the thin-film component is small and by tightly coupling it to the PCR chamber, its thermal mass can be neglected compared to the overall system. With adhesive bonding technique, the film heater can be easily integrated into different types of biochemical micro-devices such as microarray hybridization chips. Moreover, since the making of the thermal component is based on the low cost FPC mass production technology, it may find wide application in micro-fluidic systems where a precision temperature control is required.

Temperature control includes three stages: ramping-up stage, constant temperature maintaining stage and cooling stage. In the first stage, the measured temperature is lower than the set value. An H state always follows an S state. Then the transition speed is determined by the ratio of the lengths of H and S states. In the constant temperature maintaining stage, fluctuation caused by heating impulse is most concerned. The fluctuation can be minimized by shortening the length of H state, but the implementation may be limited by program and hardware speed. A reasonable length can be estimated by calculating the whole thermal capacity and the energy provided in a single H state. In cooling stage, the component is always in S state and the cooling speed is determined only by the flow rate of the forced air and the ambient temperature. Under room temperature, a box fan (12 V, 0.12 A) and a turbofan (12 V, 0.85 A) were compared, and the cooling rates were measured at 3 and 8 °C/s, respectively.

6. Conclusions

In summary, to solve the cost/fabrication problem, we have developed a thermal component acting as both a heater and a sensor using FPC technology. By following two simple control rules, temperature stability within ±0.3 °C was achieved. This system worked well with the low-voltage power supply, which makes it possible for a portable application. A PCR chip-based device was made using a piece of cover glass, plastic film and double-sided adhesive tape, and PCR reaction was successfully performed. Temperature distribution was analyzed using an FEA software, and the structural improvement was made by following the directions provided by the FEA analysis. FEA has been proved satisfactory as a powerful means in micro-system design.

Additionally, the temperature control system is not restricted to FPC components. We have designed different formats of heater/sensor components by applying the same control method. It offers an attractive way to easily integrating flexible thermal components into micro-total analysis systems (μTAS) even without micromachining techniques.

Acknowledgements

The authors would like to thank Drs. Shengce Tao, Dong Wang, Wei Shao and Wenyan Qin at National Engineering Research Center for Beijing Biochip Technology for their helpful discussions. This work was supported by the National Hi-Tech Program (no. 2002AA2Z2011) from the Department of Science and Technology, China.

References

[1] A.J. de Mello, DNA amplification: does ‘small’ really mean ‘efficient’? Lab on a Chip 1 (2001) 24N–29N.
[2] I. Schneegaß, J.M. Köhler, Flow-through polymerase chain reactions in chip thermocyclers, Rev. Mol. Biotechnol. 82 (2001) 101–121.
[3] M.A. Northrup, M.T. Ching, R.M. White, R.T. Watson, DNA amplification with a microfabricated reaction chamber, in: Proceedings

of the Seventh International Conference on Solid-state Sensors and Actuators, Yokohama, Japan, June 1993, pp. 924–926.
[4] S. Poser, T. Schulz, U. Dillner, V. Baier, J.M. Köhler, D. Schimkat, G. Mayer, A. Siebert, Chip element for fast thermocycling, Sensors Actuators A 62 (1997) 672–675.
[5] M.U. Kopp, A.J. de Mello, A. Manz, Chemical amplification: continuous-flow PCR on a chip, Science 280 (1998) 1046–1048.
[6] M.A. Shoffner, J. Cheng, G.E. Hvichia, L.J. Kricka, P. Wilding, Chip PCR. I. Surface passivation of microfabricated silicon-glass chips for PCR, Nucl. Acids Res. 24 (1996) 375–379.
[7] Y. Liu, C.B. Rouch, R.L. Stevens, R. Lenigk, J. Yang, D.B. Rhine, P. Grodzinski, DNA amplification and hybridization assays in integrated plastic monolithic devices, Anal. Chem. 74 (2002) 3063–3070.
[8] C.G. Koh, W. Tan, M. Zhao, A.J. Ricco, Z.H. Fan, Integrating polymerase chain reaction, valving, and electrophoresis in a plastic device for bacterial detection, Anal. Chem. 75 (2003) 4591–4598.
[9] Q. Zou, Y.M.Y. Chen, U. Sridhar, C.S. Chong, T. Chai, Y. Tie, C.H.L. The, T.M. Lim, C.K. Heng, Micro-assembled multi-chamber thermal cycler for low-cost reaction chip thermal multiplexing, Sensors Actuators A 102 (2002) 114–121.
[10] N.A. Friedman, D.R. Meldrum, Capillary tube resistive thermal cycling, Anal. Chem. 70 (1998) 2997–3002.
[11] Y.C. Lin, M.Y. Huang, K.C. Young, T.T. Chang, C.Y. Wu, A rapid micro-polymerase chain reaction system for hepatitis C virus amplification, Sensors Actuators B 71 (2000) 2–8.
[12] D. Pal, V. Venkataraman, A portable battery-operated chip thermocycler based on induction heating, Sensors Actuators A 102 (2002) 151–156.
[13] K. Sun, A. Yamaguchi, Y. Ishida, S. Matsuo, H. Misawa, A heater-integrated transparent microchannel chip for continuous-flow PCR, Sensors Actuators B 84 (2002) 283–289.
[14] Q. Zhang, W. Wang, H. Zhang, Y. Wang, Temperature analysis of continuous-flow micro-PCR based on FEA, Sensors Actuators B 82 (2002) 75–81.

Biographies

Keyue Shen was born in Cixi, China in 1978. He received his BEng degree from Tsinghua University in 2001. He has been studying for MS degree in the Department of Biological Sciences and Biotechnology of Tsinghua University since 2001. His research interests include bioMEMS and lab-on-a-chip systems.

Xiaofang Chen was born in Hanzhong, China in 1979. She received her BEng degree from Tsinghua University in 2001. She is pursuing MS degree in the Department of Biological Sciences and Biotechnology of Tsinghua University since 2001. Her research interests include bioMEMS and microfluids.

Min Guo received his BEng and MEng degrees from Tsinghua University in 1998 and 2001. He joined the National Engineering Research Center for Beijing Biochip Technology (NERCBBT) in 2001. He is Director of Micro-total Analysis System Department in NERCBBT. His current research interests include bioMEMS, biochip and microfluids.

Jing Cheng, PhD, is Cheung Kong Professor of Biological Sciences and Biotechnology at Tsinghua University, China, and Director of NERCBBT. Dr. Cheng received his BEng degree in Electrical Engineering from Tongji University, China, and PhD degree in Forensic Sciences from the University of Strathclyde, UK. He gained postdoc. experiences at the University of Strathclyde and the University of Aberdeen, UK, and University of Pennsylvania, USA. In 1996 he joined Nanogen Inc., as a Staff Scientist and Engineer where he was later promoted to Principal Scientist and Engineer, and Principal Investigator. From 1999 to 2001 he assumed the role of Chief Technology Officer at Aviva Biosciences Corp., USA. His current interest is in the development of microchip-based laboratory systems and ultra-high throughput drug screening systems.